

Bilthoven, Netherlands). Virus was harvested by a freeze-thaw cycle, followed by centrifugation at 680 g for 10 min. Supernatants were stored in aliquots at -80°C . Titration was performed in LLC-MK2 cells to calculate the median tissue culture infective dose (TCID₅₀) of the viral stock (18). A noninfected cell culture was used for preparation of the control inoculum. None of the stocks were contaminated by other respiratory viruses, i.e., influenza B; human parainfluenza type 1, 2, 3, 4A, and 4B; Sendai virus; respiratory syncytial virus A and B; rhinovirus; enterovirus; corona virus; and adenovirus; as determined by PCR or cell culture. Viral stock and control stock were diluted just before use in phosphate-buffered saline (PBS, pH 7.4). Primary influenza infection and secondary pneumococcal pneumonia were induced according to previously described methods (30, 31). In brief, mice were anesthetized by inhalation of isoflurane (Abbott Laboratories, Kent, UK) and intranasally inoculated with 10 TCID₅₀ influenza (1,400 viral copies) or control inoculum in a final volume of 50 μl of PBS. Pneumococcal pneumonia was induced 14 days after inoculation with influenza or control suspension. *S. pneumoniae* serotype 3 (ATCC 6303) was cultured for 16 h at 37°C in 5% CO₂ in Todd Hewitt broth. This suspension was diluted 100 times in fresh medium and grown for 5 h to midlogarithmic phase. Bacteria were harvested by centrifugation at 2,750 g for 10 min at 4°C and washed twice with ice-cold saline. After the second wash, bacteria were resuspended in saline and diluted to a concentration of 2×10^8 colony forming units (CFU) per ml, which was verified by plating out 10-fold dilutions onto blood-agar plates. Mice were anesthetized by inhalation with isoflurane and were inoculated with 50 μl of the bacterial suspension (10^8 CFU *S. pneumoniae*).

Determination of PAFR expression in the lungs. The expression of the PAFR in the lungs was determined on day 8 and day 14 after influenza virus infection. Mice (eight per time point) were anesthetized with 0.3 ml FFM (0.079 mg/ml fentanyl citrate, 2.5 mg/ml flunitasone, and 1.25 mg/ml midazolam in H₂O; of this mixture 7.0 ml/kg intraperitoneally) and killed by bleeding out the vena cava inferior. Lungs were harvested and homogenized at 4°C in four volumes of sterile saline with a tissue homogenizer (Biospec Products, Bartlesville, OK). Hundred microliters of lung homogenates were treated with 1 ml of TRIzol reagent to extract RNA. RNA was resuspended in 10 μl of diethyl pyrocarbonate-treated water. cDNA synthesis was performed using 1 μl of the RNA suspension and a random hexamer cDNA synthesis kit (Applied Biosystems, Foster City, CA). Two microliters out of 20 μl of cDNA suspension were used for amplification in real-time quantitative PCR reaction (Lightcycler Sequence Detector System; Roche, Mannheim, Germany). A standard curve was made using 10-fold dilutions of cDNA obtained from influenza virus-infected lung material. PAFR mRNA expression levels were normalized for the amount of TATA-box binding protein (TBP) mRNA present in each sample (1). The following primers were used: 5'-CTGGACCCCTAGCAGAGTTGG-3' (forward) and 5'-GCTACTCGCGATGCTGTA-3' (reverse) for PAFR, 5'-CAGGAGCCAA-GAGTGAAGAAC-3' (forward) and 5'-GGAAATAATTCTGGCT-CATAGCTACT-3' (reverse) for TBP.

Determination of viral load in the lungs. Viral load was determined on days 8 and 14 after viral infection and 48 h after pneumococcal infection (i.e., 16 days after viral infection) using real-time quantitative PCR as described (30, 31, 32). Five microliters out of 25 μl of cDNA suspension were used for amplification in a quantitative real-time PCR reaction (ABI PRISM 7700 Sequence Detector System). The viral load present in each sample was calculated with a standard curve of particle-counted influenza virus (virus particles were counted by electron microscopy), included in every assay. The following primers were used: 5'-GGACTGCAGCTGAGACGCT-3' (forward); 5'-CATCTGTGTATATGAGGCCAT-3' (reverse) and 5'-CT-CAGTTATCTGCTGCTGCACTTGC-3' (5'-FAM-labeled probe).

Determination of bacterial outgrowth. Serial 10-fold dilutions of the lung homogenates in sterile saline and 10- μl volumes were plated

out onto blood-agar plates. Plates were incubated at 37°C at 5% CO₂, and CFUs were counted after 16 h.

Histopathological analysis. Lungs for histological examination were harvested 48 h after pneumococcal infection, fixed in 10% formalin, and embedded in paraffin. Sections (4 μm) were stained with hematoxylin and eosin (H/E) and analyzed by a pathologist who was blinded for the groups.

Bronchoalveolar lavage. The trachea was exposed through a mid-line incision and cannulated with a sterile 22-gauge Abbocath-T catheter (Abbott, Sligo, Ireland). Bronchoalveolar lavage (BAL) was performed by instillation of two 0.5-ml aliquots of sterile saline into the right lung. The retrieved BAL fluid (BALF, ~ 0.8 ml) was spun at 260 g for 10 min at 4°C , and the pellet was resuspended in 0.5 ml of sterile PBS. Total cell numbers were counted using a Z2 Coulter Particle Count and Size Analyzer (Beckman-Coulter, Miami, FL). Differential cell counts were done on cytospin preparations stained with modified Giemsa stain (Diff-Quick, Baxter, UK).

Cytokine and chemokine measurements. Lung homogenates were lysed with an equal volume of lysis buffer [300 mM NaCl, 30 mM Tris, 2 mM MgCl₂, 2 mM CaCl₂, 1% (vol/vol) Triton X-100, 20 ng/ml pepstatin A, 20 ng/ml leupeptin, and 20 ng/ml aprotinin, pH 7.4] and incubated for 30 min on ice, followed by centrifugation at 680 g for 10 min. Supernatants were stored at -80°C until further use. Cytokines and chemokines in total lung lysates were measured by enzyme-linked immunosorbent assay according to the manufacturer's protocol. Reagents for interleukin (IL)-6, IL-10, cytokine-induced neutrophil chemoattractant (KC), and tumor necrosis factor (TNF)- α measurements were obtained from R&D systems (Abingdon, UK); interferon- γ reagents were obtained from Pharmingen (San Diego, CA).

Statistical analysis. All data are expressed as means \pm SE, unless stated otherwise. Differences between groups were analyzed by Mann-Whitney *U*-test. Survival was analyzed with Kaplan-Meier using a log-rank test; $P < 0.05$ was considered to represent a statistically significant difference.

RESULTS

PAFR expression in the lungs after influenza virus infection in mice. PAFR expression in the lungs was determined by real-time PCR on day 8 and day 14 after influenza virus infection. A 10-fold increase in PAFR mRNA was observed on day 8 after viral infection ($P = 0.0095$ vs. control mice, Fig. 1).

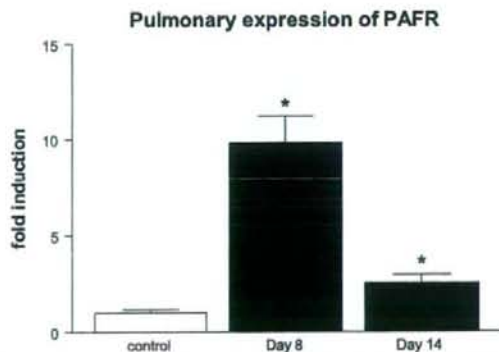


Fig. 1. Pulmonary expression of platelet-activating factor receptor (PAFR) after influenza virus infection. PAFR mRNA was measured by real-time quantitative PCR (8 mice per time point), except control group (4 mice). Expression levels were normalized for TATA-box binding protein mRNA expression levels. Data are expressed as fold induction over control (\pm SE). * $P < 0.05$ vs. control mice.

Although the expression of the PAFR declined thereafter, a 2.5-fold increase could still be observed on day 14 after viral infection ($P = 0.0162$ vs. control mice). These data indicate that influenza virus induces the expression of PAFR in vivo.

Primary influenza virus infection. Viral load in the lungs was measured on day 8 and day 14 after infection to determine the role of the PAFR during primary influenza A infection. Viral load was similar in PAFR^{-/-} and wild-type mice on day 8 after infection (Fig. 2). On day 14 after infection, both wild-type and PAFR^{-/-} mice had cleared the virus completely. These data indicate that PAFR deficiency does not hamper the clearance of influenza A in vivo.

Prolonged survival during secondary pneumococcal infection in PAFR^{-/-} mice. To investigate the role of the PAFR during secondary bacterial pneumonia we inoculated mice with *S. pneumoniae* on day 14 after influenza infection. Lethality was monitored in PAFR^{-/-} and wild-type mice (11 mice per group) during secondary pneumococcal pneumonia at least twice daily (Fig. 3). Influenza-recovered PAFR^{-/-} mice displayed a prolonged survival after pneumococcal infection ($P = 0.014$ vs. wild-type mice).

Bacterial outgrowth. To obtain insight into the role of the PAFR in the outgrowth of pneumococci in lungs previously exposed to influenza A and in the dissemination of bacteria, lungs and blood were cultured 48 h after infection with *S. pneumoniae*. The number of *S. pneumoniae* CFU was threefold lower in PAFR^{-/-} than in wild-type mice ($P = 0.05$, Fig. 4). Moreover, the PAFR played a role in the dissemination of *S. pneumoniae* into the circulation: only 57% of PAFR^{-/-} mice had positive blood cultures vs. 100% of wild-type, and the number of *S. pneumoniae* CFU in blood of PAFR^{-/-} mice was lower than in wild-type mice ($P = 0.05$, Fig. 4).

Pulmonary cytokine and chemokine concentrations. Cytokines and chemokines play an important role in host defense against bacterial pneumonia (26). Therefore, to determine the effect of the PAFR on the induction of these mediators, the concentrations of TNF- α , IL-6, IL-10, and KC were measured in lung homogenates (Fig. 5). Lung levels of TNF- α , IL-6, and IL-10 were similar in wild-type mice and PAFR^{-/-} mice on day 14 after influenza infection (Fig. 5), whereas KC produc-

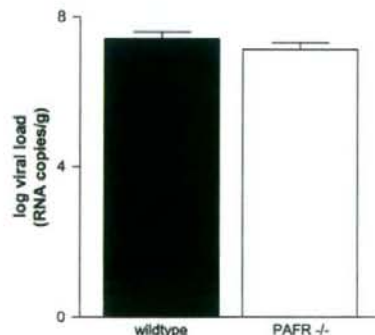


Fig. 2. Viral load in the lungs on day 8 after influenza infection. Viral load is expressed as RNA copies per gram lung tissue (means \pm SE) as determined by real-time PCR (5–8 mice per group). Both wild-type mice (filled bar) and PAFR^{-/-} mice (open bar) had cleared the virus on day 14 after infection (data not shown).

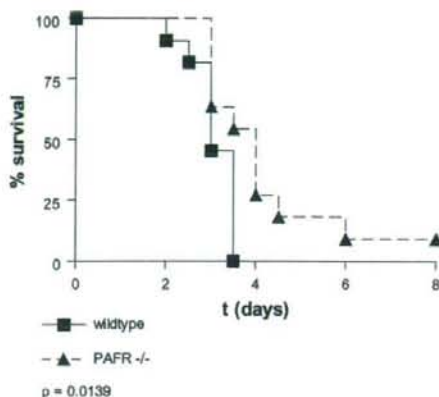


Fig. 3. Prolonged survival in PAFR^{-/-} mice after secondary bacterial pneumonia. Survival after pneumococcal infection in influenza-recovered PAFR^{-/-} mice (\blacktriangle) vs. wild-type mice (\blacksquare). All mice (11 mice per group) received 10^8 colony-forming units (CFU) of *Streptococcus pneumoniae* on day 14 after viral infection and were monitored at least twice a day after pneumococcal infection.

tion was slightly reduced in PAFR^{-/-} mice ($P = 0.0317$ vs. wild-type mice). *S. pneumoniae* infection on day 14 after influenza resulted in enhanced production of TNF- α , IL-6, IL-10, and KC (Fig. 5). On day 16, i.e., 48 h after *S. pneumoniae* infection, IL-10 and KC levels were significantly lower in PAFR^{-/-} mice than in wild-type mice ($P < 0.05$). Lung levels of TNF- α and IL-6 tended to be lower in PAFR^{-/-} mice, but the difference with wild-type mice was not statistically significant ($P = 0.16$ and $P = 0.09$ respectively).

Cell influx in BALF. Neutrophils play a pivotal role in host defense against bacterial pneumonia (26). Because inhibition of PAFR function has been shown to reduce leukocyte influx into the lungs in response to intrapulmonary delivery of killed pneumococci (16), we assessed the number of leukocytes recruited to the alveoli. Although total cell counts tended to be lower in BALF obtained from PAFR^{-/-} mice than in BALF from wild-type mice, this difference was not statistically significant. The relative number of neutrophils was trendwise lower in PAFR^{-/-} mice ($P = 0.09$ vs. wild-type mice, Table 1), whereas the relative number of macrophages was trendwise higher in PAFR^{-/-} mice ($P = 0.09$ vs. wild-type mice, Table 1).

Histopathology. Forty-eight hours after pneumococcal infection, lungs were harvested to prepare H/E-stained lung slides for histopathological examination. Mice recovered from influenza infection with secondary pneumococcal pneumonia showed severe interstitial inflammation, bronchiolitis, endothelialitis, and pleuritis in the lungs. No significant differences were observed between wild-type mice and PAFR^{-/-} mice (Fig. 6).

DISCUSSION

Secondary pneumococcal pneumonia is a serious complication of influenza A infection. The increased susceptibility to secondary bacterial infections during and shortly after influenza is, at least in part, due to enhanced colonization and interaction of the respiratory epithelium with *S. pneumoniae*

Table 1. Leukocytes in BALF 48 h after secondary bacterial pneumonia

Cells, $\times 10^3$	Wild-type Mice	PAFR ^{-/-} Mice
Total cell count	1,398 \pm 411	782 \pm 335
Neutrophils (%)	1,046 \pm 325 (67.2%)	458 \pm 184 (52.5%)
Macrophages (%)	336 \pm 98 (31.5%)	321 \pm 164 (46.8%)
Lymphocytes (%)	16.2 \pm 9.8 (1.3%)	2.9 \pm 1.5 (0.7%)

Leukocyte counts (6 mice per group) are expressed as absolute numbers ($\times 10^3$) and percentages of total cell count. All data are means \pm SE. No statistically significant differences were found between wild-type and PAFR^{-/-} mice 48 h after secondary pneumococcal pneumonia. PAFR, platelet-activating factor receptor; BALF, bronchoalveolar lavage fluid.

host previously exposed to influenza A. As such, the involvement of the PAFR in the pathogenesis of primary and postinfluenza pneumococcal pneumonia seems quite similar (20).

Of note, in our study, an interval of 14 days between viral and bacterial infection was chosen to exclude a direct interaction between influenza virus and *S. pneumoniae*. Previous studies by our group have indicated that influenza virus is completely cleared from the lungs of wild-type mice on day 14 after infection (32), which was confirmed here. The present study establishes that clearance of influenza A is not altered in PAFR^{-/-} mice: viral loads were similar in PAFR^{-/-} and wild-type mice 8 days after infection and both strains had cleared the virus completely on day 14, the day on which pneumococcal pneumonia was induced. These findings not only revealed that the PAFR does not contribute to host defense against influenza A to a significant extent but also allowed us to use PAFR^{-/-} mice to study the role of the PAFR during postinfluenza pneumococcal pneumonia.

The improved outcome observed in PAFR^{-/-} mice could also be explained by the release of protective mediators after pneumococcal infection. Pulmonary levels of KC were significantly lower in PAFR^{-/-} mice than in wild-type mice on day 14 after primary influenza infection and after secondary bacterial challenge; TNF- α and IL-6 levels were only trendwise lower. Because secondary pneumococcal infection resulted in a 100-fold increase in KC levels, it seems unlikely that the reduced KC levels on day 14 after primary influenza infection contributed to the final outcome of secondary bacterial pneumonia. The reduced KC levels after secondary bacterial infection may at least in part account for the reduced neutrophil numbers in BALF, which is line with previous studies that indicate that pulmonary KC levels correlate with neutrophil

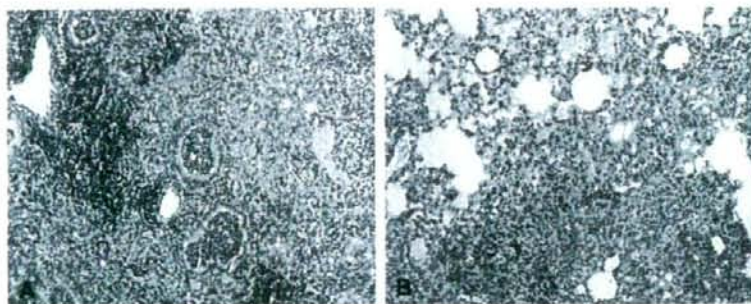
influx during *S. pneumoniae* and *P. aeruginosa* infection in mice (4, 19, 27, 29). Alternatively, and not mutually exclusive, the tendency toward a reduced inflammatory response in lungs of PAFR^{-/-} mice, which was also observed after primary pneumococcal pneumonia (20), could be the consequence of a lower bacterial load (providing a less potent proinflammatory stimulus) in the lungs (4).

We have previously shown that mice recovered from influenza produce high amounts of cytokines and excessive lung inflammation after induction of secondary pneumococcal pneumonia when compared with mice suffering from primary bacterial infection (30).

Because PAFR activation results in a proinflammatory stimulus, one could argue that the enhanced inflammatory reaction is partially due to PAFR expression in mice exposed to influenza. Indeed, the PAFR appears to be particularly important for the induction of pulmonary inflammation. Pretreatment with PAFR antagonists strongly diminished pulmonary vascular leakage and edema after systemic or intrapulmonary injection of lipopolysaccharide (13, 21, 23). Studies by Nagase et al. (15) revealed a critical role for the PAFR during acid aspiration in mice. Our current data argue against an important role for the PAFR in the exaggerated lung inflammation in mice with postinfluenza pneumonia, if one considers that PAFR^{-/-} mice only showed a tendency toward reduced levels of proinflammatory cytokines (IL-6, TNF- α) and trendwise reduced neutrophils in their lungs. Besides, pulmonary levels of the anti-inflammatory cytokine IL-10 were modestly reduced as well. Of note, in theory, the proinflammatory properties of PAF and PAF-like lipids, such as phosphorylcholine, would make these phospholipid mediators potential protective mediators during pneumonia (2). Indeed, PAFR^{-/-} mice displayed enhanced bacterial outgrowth in a mouse model for *Klebsiella pneumoniae*, a bacterium that does not express phosphorylcholine (25). This study supports the importance of phosphorylcholine binding by the PAFR during primary and secondary pneumococcal pneumonia.

S. pneumoniae is the main causative pathogen in postinfluenza pneumonia. In vitro studies have established that this bacterium can invade tissues by an interaction between phosphorylcholine present in its cell wall and the PAFR expressed by epithelial cells. We demonstrate here that the pneumococcus uses the PAFR to accomplish severe pneumonia in mice previously exposed to influenza. The fact that lethality also occurred in PAFR^{-/-} mice indicates that the PAFR is not

Fig. 6. Histopathological analysis. Inflammatory response upon pneumococcal infection in wild-type mice (A) and PAFR^{-/-} mice (B) after recovery from influenza virus. Mice received 10^4 CFU *S. pneumoniae* on day 14 after viral infection and were killed 48 h later. Lung slides were stained by hematoxylin and eosin (original magnification $\times 33$). Representative slides of 6 mice per group are shown.





mandatory for tissue invasion but, rather, that this receptor increased the potential virulence of *S. pneumoniae* in the respiratory tract. As such, the role of the PAFR in primary (20) and secondary (this study) pneumococcal pneumonia does not seem to differ significantly.

ACKNOWLEDGMENTS

We thank Joost Daalhuisen and Ingvild Kop for technical assistance during the animal experiments, Teus van den Ham for assistance during the preparation and titration of the viral stocks, and Jan Aten for the development of the quantitative PCR for TBP mRNA.

Present address of S. Ishii: Dept. of Biochemistry and Molecular Biology, Faculty of Medicine, The University of Tokyo, Tokyo, Japan.

REFERENCES

- Almeida A, Paul Thiery J, Magdelenat H, and Radvanyi F. Gene expression analysis by real-time reverse transcription polymerase chain reaction: influence of tissue handling. *Anal Biochem* 328: 101–108, 2004.
- Cabellos C, MacIntyre DE, Forrest M, Burroughs M, Prasad S, and Tuomanen E. Differing roles for platelet-activating factor during inflammation of the lung and subarachnoid space. The special case of *Streptococcus pneumoniae*. *J Clin Invest* 90: 612–618, 1992.
- Cundell DR, Gerard NP, Gerard C, Idanpaan-Heikkila I, and Tuomanen EI. *Streptococcus pneumoniae* anchor to activated human cells by the receptor for platelet-activating factor. *Nature* 377: 435–438, 1995.
- Dallaire F, Ouellet N, Bergeron Y, Turmel V, Gauthier MC, Simard M, and Bergeron MG. Microbiological and inflammatory factors associated with the development of pneumococcal pneumonia. *J Infect Dis* 184: 292–300, 2001.
- Fischer W. Phosphocholine of pneumococcal teichoic acids: role in bacterial physiology and pneumococcal infection. *Res Microbiol* 151: 421–427, 2000.
- Hirano T, Kurono Y, Ichimiya I, Suzuki M, and Mogi G. Effects of influenza A virus on lectin-binding patterns in murine nasopharyngeal mucosa and on bacterial colonization. *Otolaryngol Head Neck Surg* 121: 616–621, 1999.
- Ishii S, Kuwaki T, Nagase T, Maki K, Tashiro F, Sunaga S, Cao WH, Kume K, Fukuchi Y, Ikuta K, Miyazaki J, Kumada M, and Shimizu T. Impaired anaphylactic responses with intact sensitivity to endotoxin in mice lacking a platelet-activating factor receptor. *J Exp Med* 187: 1779–1788, 1998.
- Ishii S, Matsuda Y, Nakamura M, Waga I, Kume K, Izumi T, and Shimizu T. A murine platelet-activating factor receptor gene: cloning, chromosomal localization and up-regulation of expression by lipopolysaccharide in peritoneal resident macrophages. *Biochem J* 314: 671–678, 1996.
- Ishizuka S, Yamaya M, Suzuki T, Nakayama K, Kamanaka M, Ida S, Sekizawa K, and Sasaki H. Acid exposure stimulates the adherence of *Streptococcus pneumoniae* to cultured human airway epithelial cells: effects on platelet-activating factor receptor expression. *Am J Respir Cell Mol Biol* 24: 459–468, 2001.
- Ishizuka S, Yamaya M, Suzuki T, Takahashi H, Ida S, Sasaki T, Inoue D, Sekizawa K, Nishimura H, and Sasaki H. Effects of rhinovirus infection on the adherence of *Streptococcus pneumoniae* to cultured human airway epithelial cells. *J Infect Dis* 188: 1928–1939, 2003.
- McCullers JA and Rehg JE. Lethal synergism between influenza virus and *Streptococcus pneumoniae*: characterization of a mouse model and the role of platelet-activating factor receptor. *J Infect Dis* 186: 341–350, 2002.
- McCullers JA and Tuomanen EI. Molecular pathogenesis of pneumococcal pneumonia. *Front Biosci* 6: D877–D889, 2001.
- Miotta JM, Jeffery PK, and Hellewell PG. Platelet-activating factor plays a pivotal role in the induction of experimental lung injury. *Am J Respir Cell Mol Biol* 18: 197–204, 1998.
- Murphy BR and Webster RG. Orthomyxoviruses. In: *Fields Virology* (3rd ed.), Philadelphia, PA: Lippincott-Raven, 1996, p. 1407.
- Nagase T, Ishii S, Kume K, Uozumi N, Izumi T, Ouchi Y, and Shimizu T. Platelet-activating factor mediates acid-induced lung injury in genetically engineered mice. *J Clin Invest* 104: 1071–1076, 1999.
- O'Brien KL, Walters MI, Sellman J, Quinlisk P, Regnery H, Schwartz B, and Dowell SF. Severe pneumococcal pneumonia in previously healthy children: the role of preceding influenza infection. *Clin Infect Dis* 30: 784–789, 2000.
- Plotkowski MC, Puchelle E, Beck G, Jacquot J, and Hannoun C. Adherence of type I *Streptococcus pneumoniae* to tracheal epithelium of mice infected with influenza A/PR8 virus. *Am Rev Respir Dis* 134: 1040–1044, 1986.
- Reed LJ and Muench H. A simple method of estimating fifty percent endpoints. *Am J Hyg* 27: s493–s497, 1938.
- Remick DG, Green LB, Newcomb DE, Garg SJ, Bolgos GL, and Call DR. CXCL chemokine redundancy ensures local neutrophil recruitment during acute inflammation. *Am J Pathol* 159: 1149–1157, 2001.
- Rijnveld AW, Weijer S, Florquin S, Speelman P, Shimizu T, Ishii S, and van der Poll T. Improved host defense against pneumococcal pneumonia in platelet-activating factor receptor-deficient mice. *J Infect Dis* 189: 711–716, 2004.
- Rylander R, Beijer L, Lantz RC, Burrell R, and Sedivy P. Modulation of pulmonary inflammation after endotoxin inhalation with a platelet-activating factor antagonist (48740 RP). *Int Arch Allergy Appl Immunol* 86: 303–307, 1988.
- Shirasaki H, Nishikawa M, Adcock IM, Mak JC, Sakamoto T, Shimizu T, and Barnes PJ. Expression of platelet-activating factor receptor mRNA in human and guinea pig lung. *Am J Respir Cell Mol Biol* 10: 533–537, 1994.
- Stiebeck M, Weipert J, Keser C, Kohl J, Spannagl M, Machleidt W, and Schweiberer L. A triazolodiazepine platelet activating factor receptor antagonist (WEB 2086) reduces pulmonary dysfunction during endotoxin shock in swine. *J Trauma* 31: 942–949, 1991.
- Simon HU, Tsao PW, Simionovitch KA, Mills GB, and Blaser K. Functional platelet-activating factor receptors are expressed by monocytes and granulocytes but not by resting or activated T and B lymphocytes from normal individuals or patients with asthma. *J Immunol* 153: 364–377, 1994.
- Soares AC, Pinho VS, Souza DG, Shimizu T, Ishii S, Nicoli JR, and Teixeira MM. Role of the platelet-activating factor (PAF) receptor during pulmonary infection with gram negative bacteria. *Br J Pharmacol* 137: 621–628, 2002.
- Strieter RM, Belperio JA, and Keane MP. Cytokines in innate host defense in the lung. *J Clin Invest* 109: 699–705, 2002.
- Tateda K, Moore TA, Newstead MW, Tsai WC, Zeng X, Deng JC, Chen G, Reddy R, Yamaguchi K, and Standiford TJ. Chemokine-dependent neutrophil recruitment in a murine model of *Legionella pneumoniae*: potential role of neutrophils as immunoregulatory cells. *Infect Immun* 69: 2017–2024, 2001.
- Treanor JJ. Orthomyxoviridae: influenza virus. In: *Principles and Practice of Infectious Diseases* (5th ed.), New York: Churchill Livingstone, 2000, p. 1834–1835.
- Tsai WC, Strieter RM, Mehrad B, Newstead MW, Zeng X, and Standiford TJ. CXCL chemokine receptor CXCR2 is essential for protective innate host response in murine *Pseudomonas aeruginosa* pneumonia. *Infect Immun* 68: 4289–4296, 2000.
- Van Elden LJR, Nijhuis M, Schipper P, Schuurman R, and van Loon AM. Simultaneous detection of influenza virus A and B using real-time quantitative PCR. *J Clin Microbiol* 39: 196–200, 2001.
- Van der Stuijts KF, Van Elden L, Nijhuis M, Schuurman R, Florquin S, Jansen HM, Lutter R, and Van der Poll T. Toll-like receptor 4 is not involved in host defense against respiratory tract infection with Sendai virus. *Immunol Lett* 89: 201–206, 2003.
- Van der Stuijts KF, Van Elden LJR, Nijhuis M, Schuurman R, Pater JM, Florquin S, Goldman M, Jansen HM, Lutter R, and Van der Poll T. IL-10 is an important mediator of the enhanced susceptibility to pneumococcal pneumonia after influenza infection. *J Immunol* 172: 7603–7609, 2004.

Cardiovascular, Pulmonary and Renal Pathology

Attenuation of Folic Acid-Induced Renal Inflammatory Injury in Platelet-Activating Factor Receptor-Deficient Mice

Kent Doi,* Koji Okamoto,* Kousuke Negishi,*
Yoshifumi Suzuki,* Akihide Nakao,*
Toshiro Fujita,* Akiko Toda,*†
Takehiko Yokomizo,† Yoshihiro Kita,†
Yasuyuki Kihara,† Satoshi Ishii,† Takao Shimizu,††
and Eisei Noiri*‡

From the Departments of Nephrology and Endocrinology,* and
Biochemistry and Molecular Biology,¹ and the Center for
NanoBio Integration,² University of Tokyo, Tokyo, Japan

Platelet-activating factor (PAF), a potent lipid mediator with various biological activities, plays an important role in inflammation by recruiting leukocytes. In this study we used platelet-activating factor receptor (PAFR)-deficient mice to elucidate the role of PAF in inflammatory renal injury induced by folic acid administration. PAFR-deficient mice showed significant amelioration of renal dysfunction and pathological findings such as acute tubular damage with neutrophil infiltration, lipid peroxidation observed with antibody to 4-hydroxy-2-hexenal (day 2), and interstitial fibrosis with macrophage infiltration associated with expression of monocyte chemoattractant protein-1 and tumor necrosis factor- α in the kidney (day 14). Acute tubular damage was attenuated by neutrophil depletion using a monoclonal antibody (RB6-8C5), demonstrating the contribution of neutrophils to acute phase injury. Macrophage infiltration was also decreased when treatment with a PAF antagonist (WEB2086) was started after acute phase. *In vitro* chemotaxis assay using a Boyden chamber demonstrated that PAF exhibits a strong chemotactic activity for macrophages. These results indicate that PAF is involved in pathogenesis of folic acid-induced renal injury by activating neutrophils in acute phase and macrophages in chronic interstitial fibrosis. Inhibiting the PAF pathway might be therapeutic to kidney injury from inflammatory cells. (*Am J Pathol* 2006; 168:1413-1424; DOI: 10.2353/ajpath.2006.050634)

Inflammation is an important component of renal injury, in both acute renal failure^{1,2} and chronic renal damage that accompanies interstitial fibrosis.^{3,4} The infiltrating inflammatory cells contribute to renal damage through generation of reactive oxygen species (ROS), further recruitment of leukocytes, and production of proinflammatory and profibrotic cytokines. Therefore, the mechanism of directing circulating leukocytes to the kidney and maintaining them there is a potential target for therapeutic intervention for kidney diseases.

Platelet-activating factor (PAF; 1-O-alkyl-2-acetyl-sn-glycero-3-phosphocholine) is a potent proinflammatory phospholipid mediator with various biological effects such as activating platelets, neutrophils, eosinophils, and macrophages. PAF binds to a G-protein-coupled seven transmembrane receptor, PAF receptor (PAFR); PAF plays an important role in the pathophysiology of inflammatory conditions.^{5,6} Synthesis of PAF has been demonstrated not only in blood cells but in the kidney under physiological conditions,⁷ ischemia reperfusion injury,⁸ and clipped kidney.⁹ Treatment with several PAF antagonists has been reported in acute renal failure¹⁰ and chronic renal failure animal models.^{11,12} However, problems exist regarding the lack of specificity of PAF antagonists.¹³⁻¹⁶ Therefore, we have developed genetically engineered PAFR-deficient (PAFR-KO) mice to confirm the role of PAF *in vivo*.¹⁷ The resultant PAFR-KO mice exhibit attenuated symptoms in several animal models such as chemical lung injury,¹⁸ bronchial asthma,¹⁹ and sponge-induced subcutaneous granuloma formation.²⁰ It

Supported in part by grants from the Cell Science Research Foundation, Osaka, Japan (to E.N.); the Araki Memorial Research Foundation for Medicine and Biochemistry, Tokyo, Japan (to E.N.); Takeda Medical Science, Osaka, Japan (to E.N.); and the Health and Labour Science research grants for Research on Human Genome, Tissue Engineering, and Food Biotechnology from the Ministry of Health, Labour, and Welfare of Japan (to E.N.).

K.D. and K.O. contributed equally to this work.

Accepted for publication January 10, 2006.

Address reprint requests to Dr. Eisei Noiri, M.D., Ph.D., Department of Nephrology and Endocrinology, University of Tokyo, 7-3-1 Hongo, Bunkyo, Tokyo 113-8655, Japan. E-mail: noiri-ky@umin.ac.jp.

has been demonstrated that infiltrating inflammatory cells play important roles in these animal models.

The folic acid (FA)-induced renal injury model has been applied recently for evaluation of epithelial regeneration and interstitial fibrosis.²¹⁻²⁴ Intraperitoneal administration of FA with sodium bicarbonate induced renal injury that showed acute tubular necrosis with transient elevations of blood urea nitrogen (BUN) and serum creatinine (Cr) followed by development of interstitial fibrosis with macrophage infiltration.²¹⁻²⁵ Tubular obstructions by FA crystals and direct toxic effect of FA to tubular epithelial cells presumably cause renal damage,²⁶ but the precise mechanism of injury remains unclear. Inflammatory cell infiltrations were remarkable in injured kidneys of this model.

Here we examined the role of PAF in inflammatory renal injury induced by FA administration. Using PAFR-KO mice, we show attenuation of renal injury not only in cases of acute tubular damage but also in cases of development of chronic interstitial fibrosis *in vivo*. In addition, we evaluated the effects of neutrophil depletion and PAF antagonist treatment after the acute phase to confirm the contribution of leukocytes to FA-induced renal injury. We also demonstrate the role of PAF as a strong chemoattractant for macrophages *in vitro*, indicating that PAF blockade can prevent progression of inflammatory damage in kidney.

Materials and Methods

Reagents

Folic acid was obtained from Sigma Chemical Co. (St. Louis, MO) and WEB2086 was a generous gift from Boehringer (Ingelheim, Germany). We used a mouse antibody to 4-hydroxy-2-hexenal (HHE)-modified protein, in which the aldehyde HHE is derived from the oxidative process of polyunsaturated fatty acid, obtained from NOF Corp. (Tokyo, Japan) and a mouse anti-smooth muscle α actin (α -SMA) monoclonal antibody (1A4) (DakoCytomation Co. Ltd., Glostrup, Denmark) for immunohistochemical and Western blot analyses. We used a rat anti-mouse neutrophil antibody (Caltag Laboratories, Burlingame, CA), a rat anti-mouse F4/80 macrophage antigen antibody (MCA497R) (Serotec, Raleigh, NC), and a goat anti-mouse MCP-1/JE antibody (Santa Cruz Biotechnology Inc., Santa Cruz, CA) for immunohistochemical analyses. The monoclonal antibody RB6-8C5 was used for neutrophil depletion. It is a rat IgG2b that selectively binds to and depletes mature neutrophils but not lymphocytes or macrophages.²⁷⁻³¹ The hybridoma that secretes this antibody was a gift from Dr. R. Coffman (DNAX Research Inc., Palo Alto, CA); RB6-8C5 from hybridoma culture supernatants was purified through ammonium sulfate precipitation. All other chemicals were purchased from Wako Pure Chemical Industries Ltd. (Osaka, Japan) unless otherwise specified.

Animal Model

We established PAFR-KO mice as described previously.¹⁷ The PAFR-KO mice and the corresponding wild-type (PAFR-WT) mice were backcrossed for 10 generations onto a C57BL/6N genetic background. Mice were allowed food and water *ad libitum*, and experiments were conducted in accordance with the Guide for the Care and Use of Laboratory Animals [Department of Health, Education and Welfare Publication No. (NIH) 86-23, Revised 1985, Office of Science and Health Reports, DRR/NIH, Bethesda, MD]. Male and female mice used for this study were 9 to 11 weeks of age, weighing 18 to 25 g. Within each experimental group, the sex ratio, age, and weight of animals did not differ significantly. The animals were anesthetized with diethyl ether and administered FA by intraperitoneal injection at the dose of 250 mg/kg in vehicle (0.5 ml of 0.3 mmol/L NaHCO₃) or given vehicle alone. The dose of FA and NaHCO₃ was critical for induction of severe renal damage and was determined by preliminary studies. Blood was drawn from the tail vein of each animal, and the levels of BUN and Cr were measured 3 days before and at 2, 7, and 14 days after FA administration by the urease-indophenol method with Urea N B (Wako Pure Chemical Industries Ltd.) and the colorimetric method based on hydrogen peroxide measurement with Nescoat VLI CRE (Alfresa Pharma Corp., Osaka, Japan), respectively. Kidneys were removed 2 and 14 days after FA administration and fixed in 10% buffered formalin for staining with hematoxylin and eosin, Masson's trichrome, and immunochemical staining, except for mouse neutrophil detection for which methyl Carnoy's solution was used. Parts of kidneys were snap-frozen for immunohistochemical testing of MCP-1; they were otherwise used for Western blot analysis and real-time polymerase chain reaction (PCR) assay.

For neutrophil depletion experiments, PAFR-WT mice were treated with 50 μ g of monoclonal antibody RB6-8C5. Injection of FA was performed the following day, and the animals were sacrificed 2 days after FA administration. Injection of 25 μ g of monoclonal antibody RB6-8C5 was reported to cause significant neutrophil depletion from the subsequent day up to 3 days.³²⁻³⁴ Blood collected at sacrifice was used for flow cytometry analyses to confirm neutrophil depletion. Mice that were untreated with RB6-8C5 served as control animals. To clarify the contribution of PAF for macrophage recruitment after initial damage, we intraperitoneally injected PAF antagonist (WEB2086) into PAFR-WT mice every day from day 2 to day 14 at the dose of 5 mg/kg and examined renal function (days 2, 7, and 14), macrophage infiltration, and interstitial fibrosis (day 14).

Flow Cytometry Analysis

Heparinized blood was incubated with anti-Gr-1 antibodies conjugated to fluorescein isothiocyanate (BD Pharmingen, San Diego, CA), and then Flowcount fluorospheres (Beckman Coulter Inc., Villepinte, France) were added. After red blood cell lysis with NH₄Cl buffer, cell suspen-

sion was run on a FACScan flow cytometer (Becton Dickinson Immunocytometry Systems, San Jose, CA), and the absolute count of Gr-1-positive cells was calculated using standardized Flowcount beads.

Morphological Evaluation of Kidneys

The area of the interstitial fibrosis in the cortex was evaluated with Masson's trichrome staining using a computer-aided evaluation program (AIS version 4.0; Fuji Photo Film Co. Ltd., Tokyo, Japan). Viewed at $\times 400$ magnification, 10 randomly selected nonoverlapping fields from the cortical region were analyzed. The fibrotic areas stained in blue were depicted in digital images; then the percentage of the fibrotic area was calculated relative to the entire field area (percentage area). Glomeruli and large vessels were not included in the microscopic fields for image analysis. The degree of neutrophil and macrophage infiltration was measured as the average number of positive staining cells per field. The number of positively stained cells was determined in five randomly selected nonoverlapping fields at $\times 200$ magnification in each section of the individual mouse renal cortex. Scores of respective kidneys as well as scores of each animal were averaged.

Western Blot Analysis

Western blot analyses were performed as described previously.³⁵ Briefly, harvested kidneys were homogenized on ice in a radioimmunoprecipitation assay buffer with protease inhibitors. The lysates were separated electrophoretically on a 10% polyacrylamide gel. After transferring proteins from the gel to a nitrocellulose membrane, Western blot analyses were performed using HHE or α -SMA antibody. After incubation with horseradish peroxidase-conjugated appropriate second antibody, chemiluminescent signal detection (ECL Plus; Amersham Biosciences Corp., Uppsala, Sweden) was performed using a cooled charge-coupled device camera system (LAS-1000; Fuji Photo Film Co. Ltd.). The membrane was incubated at 50°C for 30 minutes in a stripping buffer to remove all probes. Then it was re probed with the antibody to α -tubulin (Santa Cruz Biotechnology Inc.). Densitometric analyses of bands compared with the density of α -tubulin were performed using National Institutes of Health Image software, version 1.62.

Immunohistochemical Analysis

Immunohistochemical staining of 2- μ m paraffin sections was performed using indirect immunohistochemical techniques. Biotin-free immunohistochemical staining using horseradish peroxidase-conjugated polymer system was conducted according to the manufacturer's protocols (Histofine Mouse Stain kit and Histofine Simple Stain mouse MAX-PO (rat) kit; Nichirei Corp., Tokyo, Japan). The deparaffinized sections were preincubated with 0.3% hydrogen peroxide for 15 minutes and incubated with primary antibodies overnight at 4°C, followed by

polymer-conjugated anti-mouse IgG. Protease K treatment was necessary for anti-F4/80 antibody; autoclaving in 10 mmol/L citrate-buffer (pH 6.0) was necessary for anti-HHE and anti- α -SMA antibody. For neutrophil staining, fixation with methyl Carnoy's solution was indispensable.³⁶ Diaminobenzidine tetrahydrochloride (Nichirei Corp.) was used for the substrate-chromogen reaction followed by counter staining with hematoxylin.

We used frozen sections of kidney to determine the immunohistochemistry of MCP-1, as described previously³⁷ but with modifications. With 8- μ m cryostat sections fixed in acetone and goat anti-mouse MCP-1 antibody (Santa Cruz Biotechnology Inc.), a Vectastain Elite ABC kit (Vector Laboratories Inc., Burlingame, CA) and diaminobenzidine tetrahydrochloride were applied in accordance with the manufacturers' instructions. Sections were counterstained with methyl green (Vector Laboratories Inc.).

Real-Time PCR Assay for TNF- α and MCP-1 Expression

Harvested kidneys were homogenized with a homogenizer (Ultra-Turrax T8; IKA Labortechnik, Staufen, Germany) in Trizol total RNA isolation reagent (Invitrogen Corp., Carlsbad, CA). Total RNA was isolated by the acid guanidinium isothiocyanate-phenol-chloroform extraction method according to the manufacturer's protocols and treated with DNase I to remove potential contamination of DNA (DNA-free; Ambion Inc., Austin, TX). The mRNA was then reverse-transcribed to cDNA using MLV reverse transcriptase (RiverTra Ace; Toyobo Co. Ltd., Osaka, Japan) with random hexamers. Transcripts encoding tumor necrosis factor (TNF)- α and monocyte chemoattractant protein (MCP)-1 were measured using TaqMan real-time quantitative PCR with Prism 7000 sequence detection system (Applied Biosystems, Foster City, CA) using TaqMan universal PCR master mix (Applied Biosystems) according to the manufacturer's specifications. The TaqMan probes and primers for TNF- α (assay identification number Mm00443258.m1) and MCP-1 (assay identification number Mm00441242.m1) were assay-on-demand gene expression products (Applied Biosystems). The PCR reaction conditions were 95°C for 10 minutes, followed by 40 cycles of 95°C for 15 seconds and 60°C for 1 minute. To normalize for variance in loaded cDNA, 18S ribosomal RNA were amplified in a separate tube. Amplification data were analyzed using Applied Biosystems' Prism sequence detection software version 2.1 (Applied Biosystems). Standard curves were prepared for each gene and the 18S ribosomal RNA in each experiment to normalize the relative expression of the genes of interest to the 18S ribosomal RNA control.

Measurement of PAF Levels in Kidney

Harvested kidneys were frozen immediately with liquid nitrogen at days 2 and 14. The PAF levels in kidney were measured by reverse-phase high performance liquid chromatography-electrospray ionization-tandem mass

spectrometry technique, as described in precedent studies.^{38,39}

Migration Assay

Elicited peritoneal macrophages were harvested from PAFR-KO and PAFR-WT mice 3 days after injection of 4% thioglycolate. Peritoneal exudate cells were washed with phosphate-buffered saline and resuspended in RPMI 1640 medium supplemented with 0.1% bovine serum albumin. Cell migration was evaluated using a 96-well Boyden chamber as described previously, with minor modifications.⁴⁰ The PAF at concentrations of 0, 1, and 10 nmol/L in 300 μ l of RPMI 1640 containing 0.1% bovine serum albumin was added to the lower wells of a chemotaxis chamber (Neuro Probe, Inc., Gaithersburg, MD). A polycarbonate filter (8- μ m-pore size; Neuro Probe, Inc.) was layered onto the wells; 65 μ l of cell suspension (4.0×10^6 /ml) were applied to the upper wells. The chamber was incubated at 37°C in a humidified atmosphere in the presence of 5% CO₂ for 2 hours. At the end of incubation, the filter was removed, fixed with methanol, and stained with Diff-Quick (Sysmex Corp., Hyogo, Japan). Cells on the upper side of the filter were wiped away. The number of cells that had migrated to the lower side was determined by measuring optical densities at 595 nm using a 96-well microplate reader (model 3550; Bio-Rad Laboratories Inc., Hercules, CA). Each experiment was performed in triplicate.

Statistical Analysis

Results of statistical analyses are expressed as means \pm SEM. Differences among groups at the same time point were examined using Student's *t*-test. Differences among experimental groups at different time point were confirmed by one-way analysis of variance followed by the Tukey-Kramer test for individual comparison of group means. These calculations were performed using StatView-J5.0 (SAS Institute Inc., Cary, NC). The null hypothesis was rejected when *P* was <0.05.

Results

Attenuation of Renal Dysfunction in PAFR-KO Mice and Efficacy of PAFR Antagonist

Administration of FA with sodium bicarbonate induced transient elevation of BUN and Cr at 48 hours after injection followed by subsequent renal dysfunction accompanied with interstitial fibrosis. Basal levels of BUN and Cr in PAFR-WT and PAFR-KO mice were similar [PAFR-WT: BUN 28.1 ± 0.8 mg/dl, Cr 0.25 ± 0.01 mg/dl (*n* = 16) versus PAFR-KO: BUN 27.8 ± 0.9 mg/dl, Cr 0.24 ± 0.01 mg/dl (*n* = 16)]. The measurement at 48 hours after FA injection showed statistically significant elevation of BUN and Cr compared with baseline in both PAFR-WT and PAFR-KO mice (PAFR-WT, *P* < 0.001; PAFR-KO, *P* < 0.005), and the levels of

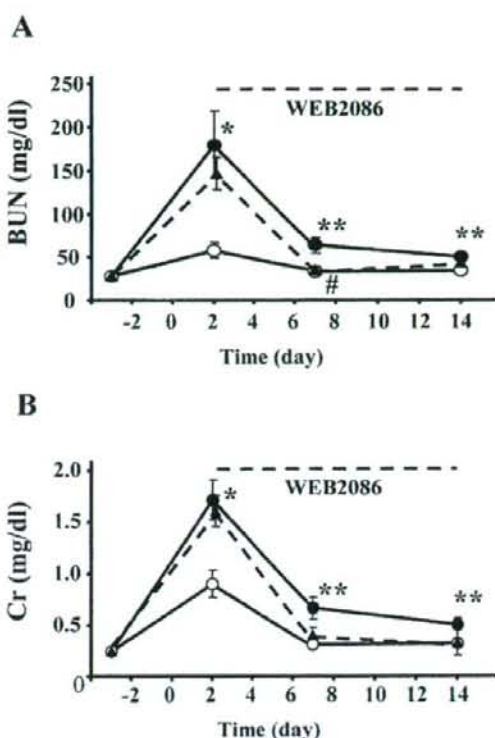


Figure 1. Time course of BUN (A) and Cr (B) levels in PAFR-KO and PAFR-WT mice subjected to FA administration. Filled circles indicate PAFR-WT mice, open circles indicate PAFR-KO mice, and filled triangles indicate WEB2086-treated PAFR-WT mice. WEB2086 was injected every day from days 2 to 14. The numbers of animals were 16 at days -3 and 2, 8 at days 7 and 14 in PAFR-WT and PAFR-KO mice, and 5 in WEB2086-treated PAFR-WT mice. **P* < 0.005, ***P* < 0.05 (PAFR-WT versus PAFR-KO). #*P* < 0.05 (PAFR-WT versus WEB2086-treated PAFR-WT).

BUN and Cr in PAFR-WT mice were significantly higher compared with levels in PAFR-KO mice [PAFR-WT: BUN 180.0 ± 39.0 mg/dl, Cr 1.71 ± 0.20 mg/dl (*n* = 16) versus PAFR-KO: BUN 58.2 ± 8.9 mg/dl, Cr 0.90 ± 0.13 mg/dl (*n* = 16); *P* < 0.005] (Figure 1). The significant differences were also valid at days 7 and 14 [PAFR-WT: BUN 63.7 ± 9.4 mg/dl, Cr 0.66 ± 0.11 mg/dl (*n* = 8) versus PAFR-KO: BUN 33.1 ± 3.3 mg/dl, Cr 0.31 ± 0.04 mg/dl (*n* = 8); *P* < 0.05, at day 7] [PAFR-WT: BUN 50.2 ± 5.2 mg/dl, Cr 0.50 ± 0.06 mg/dl (*n* = 8) versus PAFR-KO: BUN 33.8 ± 3.3 mg/dl, Cr 0.31 ± 0.04 mg/dl (*n* = 8); *P* < 0.05, at day 14]. Treatment with WEB2086 after acute phase from day 2 to day 14 also showed partial protective effects for renal dysfunction [day 2: BUN 146.9 ± 18.7 mg/dl, Cr 1.60 ± 0.15 mg/dl; day 7: BUN 35.5 ± 3.6 mg/dl, Cr 0.39 ± 0.07 mg/dl; day 14: BUN 43.4 ± 3.9 mg/dl, Cr 0.32 ± 0.12 mg/dl (*n* = 5)]. In addition, there was a significant difference between WEB2086-treated and untreated PAFR-WT mice in BUN level at day 7 (*P* < 0.05) (Figure 1).

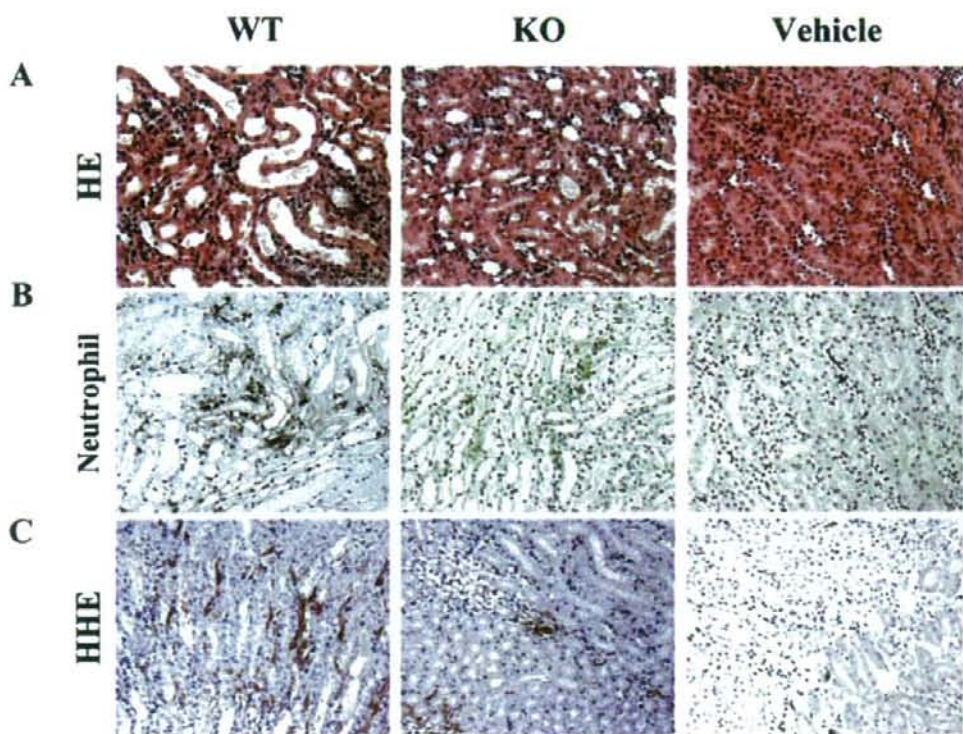


Figure 2. Histological findings at day 2 stained with H&E (A), immunohistochemistry using antibody to neutrophil (B), and antibody to HHE-modified proteins (C). Vehicle-treated PAFR-KO and PAFR-WT showed identical results. Therefore, only PAFR-WT mice are shown. Original magnifications, $\times 200$.

Neutrophil and ROS Production in Acute Tubular Damage

In addition to attenuation of renal dysfunction, morphological analyses demonstrated that acute tubular necrosis was significantly milder in PAFR-KO mice than in PAFR-WT mice at 48 hours after FA administration (Figure 2A). Immunohistochemical staining with anti-neutrophil antibody showed that infiltrating neutrophils decreased significantly in PAFR-KO mice compared with PAFR-WT mice at day 2 [PAFR-WT: $27.5 \pm 2.3/\times 200$ field ($n = 4$) versus PAFR-KO: $6.9 \pm 1.0/\times 200$ field ($n = 4$); $P < 0.001$] and were detected predominantly around the damaged tubules (Figure 2B and Figure 3).

Through propagation of lipid peroxidation, ROS will damage tissue. Antibody to HHE, produced in the oxidative metabolism of ω -3 polyunsaturated fatty acids in cell membranes, is a specific marker to detect lipid peroxidation.³⁵ Immunohistochemical analyses dominantly detected HHE-modified proteins around peritubular capillaries of damaged kidney tissues (Figure 2C). Lipid peroxidation was also quantified in kidney homogenates by Western blot analysis. In PAFR-WT mice, kidney homogenates showed a higher intensity of immunoreactive bands of HHE-modified proteins compared with those from PAFR-KO mice (Figure 4).

To evaluate the contribution of neutrophils for acute phase of FA-induced renal injury at day 2, we also injected FA into PAFR-WT mice pretreated with neutrophil depletion antibody. Neutrophil depletion was confirmed through flow cytometry analyses (Figure 5A). These ani-

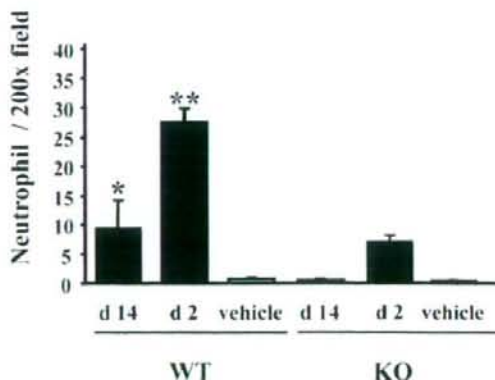


Figure 3. Number of infiltrating neutrophils in FA-injured kidney. Five animals were in the FA group; four received the vehicle. * $P < 0.005$ versus PAFR-KO mice at day 14 (d 14). ** $P < 0.00005$ versus PAFR-KO mice at day 2 (d 2).

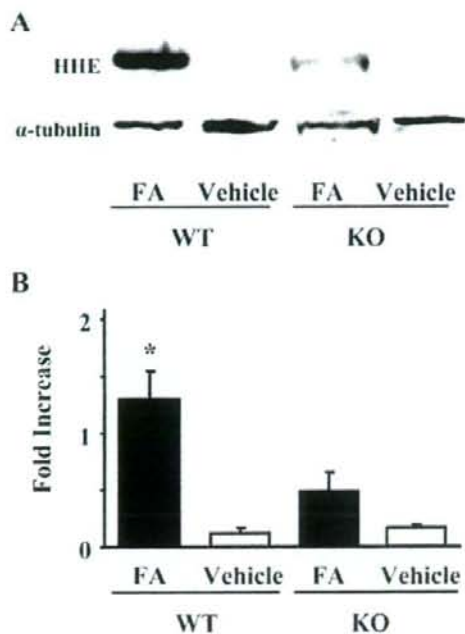


Figure 4. Western blot analysis of HHE-modified protein expression in kidney homogenates at day 2. A representative image is shown in **A** (top). **B:** The histogram depicts the relative density of bands in comparison with α -tubulin. Five animals were in the FA group; three received the vehicle. * $P < 0.05$ versus PAFR-KO mice with FA administration.

mals showed remarkable amelioration of renal dysfunction [control: BUN 133.5 ± 21.1 mg/dl, Cr 1.54 ± 0.09 mg/dl ($n = 5$) versus neutrophil depletion: BUN 35.3 ± 2.4 mg/dl, Cr 0.47 ± 0.16 mg/dl ($n = 5$); $P < 0.005$] (Figure 5, B and C).

Development of Interstitial Fibrosis and Macrophage Infiltration

The FA-induced renal injury model showed development of segmental interstitial fibrotic lesions at day 14. Figure 6A shows that interstitial fibrotic areas stained in blue by Masson's trichrome staining were more prominent in kidneys of PAFR-WT mice than in those of PAFR-KO mice. Quantitative analyses demonstrated that the fibrotic area in PAFR-WT mice was significantly larger than PAFR-KO mice [PAFR-WT: $5.4 \pm 0.7\%$ ($n = 5$) versus PAFR-KO: $2.1 \pm 0.7\%$ ($n = 5$); $P < 0.05$] (Figure 7). Immunohistochemical and Western blot analyses with anti- α -SMA antibody were performed to detect interstitial myofibroblasts. Positive staining of α -SMA was found in the identical site of fibrotic area stained blue with Masson's trichrome staining (Figure 6B) and seen in vascular smooth muscle cells (data not shown). Kidney homogenates of PAFR-WT mice were shown by Western blot analysis to have a higher intensity of immunoreactive bands of α -SMA than those from PAFR-KO mice (Figure 8).

Macrophage infiltration was evaluated using immunostaining for F4/80, a specific macrophage antigen. Infil-

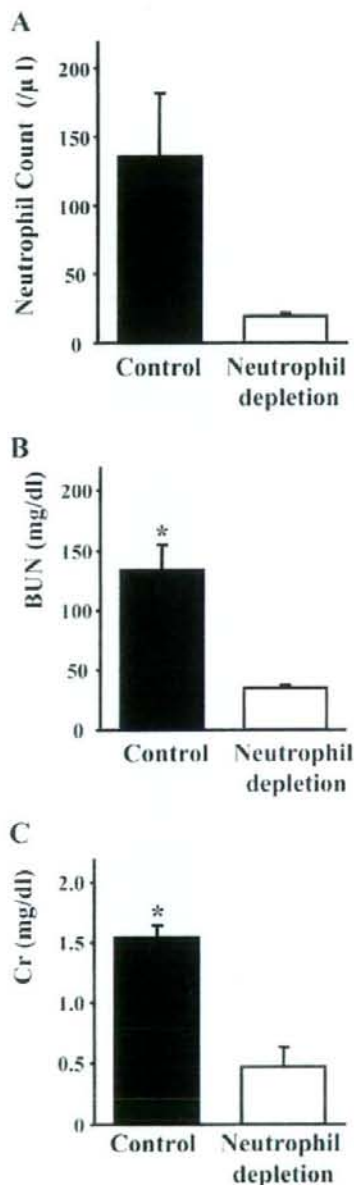


Figure 5. Effects of neutrophil depletion on acute phase of FA-induced renal injury. Injection of a monoclonal neutrophil depletion antibody (RB6-8C5) at day -1 caused a significant decrease of neutrophil count in blood of PAFR-WT mice at day 2. **A:** Renal dysfunction at day 2 was attenuated with treated PAFR-WT mice compared with untreated PAFR-WT mice (**B** and **C**). * $P < 0.005$ versus untreated PAFR-WT mice. Five animals were in each group.

trated F4/80-positive macrophages were detected in the peritubular interstitium around fibrotic areas in kidneys harvested 14 days after FA administration (Figure 6C). The number of infiltrated F4/80-positive macrophages at

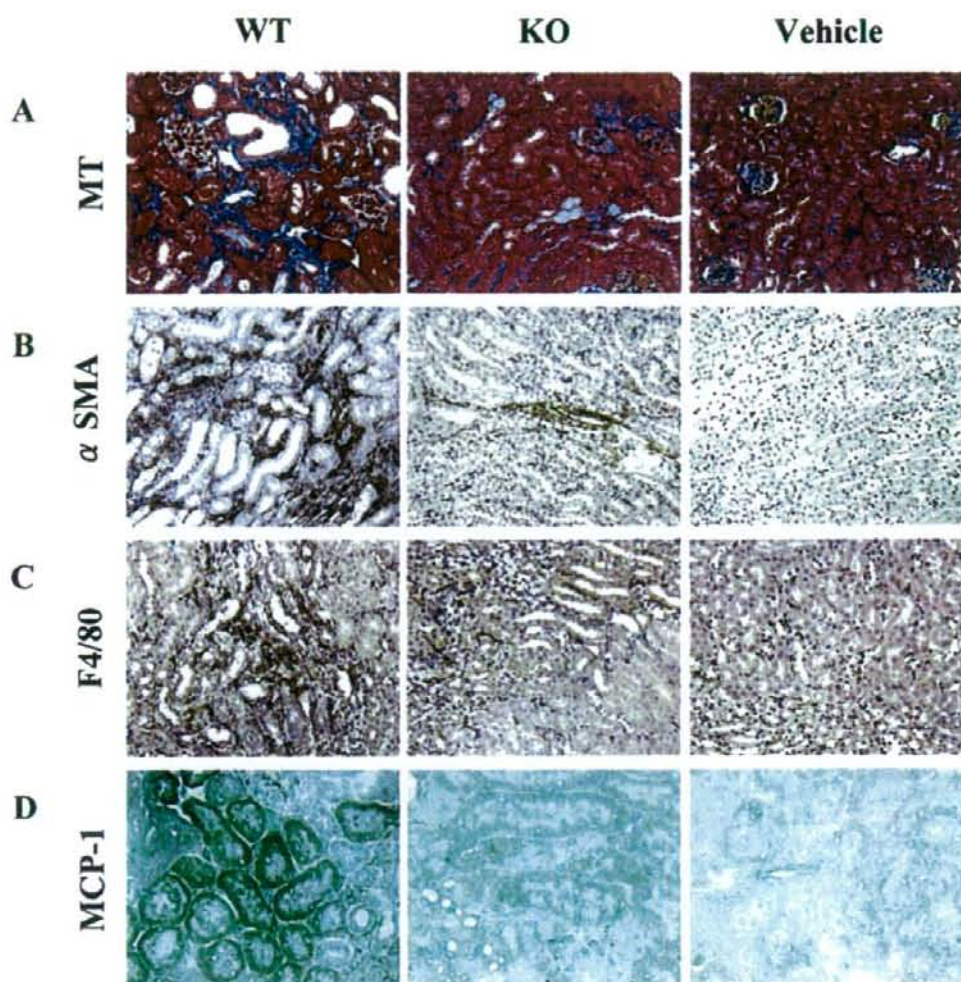


Figure 6. Histological findings at day 14 stained with Masson's trichrome (A), immunohistochemistry using antibody to α -SMA (B), antibody to F4/80-positive macrophage (C), and immunohistochemical analyses using antibody to MCP-1 with frozen sections. Vehicle-treated PAFR-KO and PAFR-WT showed identical results. Therefore, only PAFR-WT mice results are shown. Original magnifications: $\times 100$ (A); $\times 200$ (B, C); $\times 400$ (D).

day 14 in PAFR-WT mice was significantly higher than that in PAFR-KO mice [PAFR-WT: $97.5 \pm 11.9/\times 200$ field ($n = 5$) vs. PAFR-KO: $32.1 \pm 8.6/\times 200$ field ($n = 5$); $P < 0.05$] (Figure 9). In contrast, the numbers of F4/80-positive cells in kidneys harvested at 48 hours after FA administration did not differ among groups [PAFR-WT: $28.5 \pm 6.7/\times 200$ field ($n = 5$) versus PAFR-KO: $18.7 \pm 2.0/\times 200$ field ($n = 5$); $P = 0.21$].

The PAFR-WT mice treated with WEB2086 after acute phase every day (from day 2 to day 14) showed significantly decreased interstitial fibrosis and macrophage infiltration at day 14 compared with untreated PAFR-WT mice [fibrotic area: $3.5 \pm 0.3\%$ ($n = 5$); $P < 0.05$ versus untreated PAFR-WT mice and macrophage counts;

$66.0 \pm 6.3/\times 200$ field ($n = 5$); $P < 0.05$ versus untreated PAFR-WT mice] (Figures 7 and 9).

TNF- α and MCP-1 Expression in FA-Induced Renal Injury

We examined TNF- α and MCP-1 mRNA expression using TaqMan real-time PCR assay to confirm the contribution of macrophages for FA-induced renal injury. Decreased expression of both TNF- α and MCP-1 were shown in the kidney of PAFR-KO mice compared with PAFR-WT mice (Figure 10). Furthermore, increased expression of these cytokines at day 14 was found only in PAFR-WT mice.

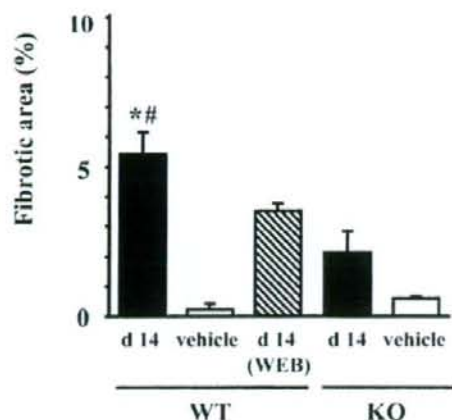


Figure 7. The fibrotic area in the cortex from the kidney at day 14 (d 14) was calculated using a computer-aided evaluation program. Five animals were in the FA group, four received the vehicle. * $P < 0.05$ versus PAFR-KO mice. * $P < 0.05$ versus PAFR-KO mice with FA administration. * $P < 0.05$ versus WT32885-treated PAFR-WT mice.

These results indicate that macrophage accumulation to the injured kidney was amplified even after acute tubular damage at day 2. In addition, immunohistochemical analysis at day 14 revealed that MCP-1 protein was expressed dominantly in the proximal tubular epithelium (Figure 6D).

PAF Levels in Kidney

To clarify the presence of PAF and PAFR pathway in FA-induced renal injury, we examined the levels of PAF in the kidney. The renal PAF levels were virtually the same in normal kidney of PAFR-KO and PAFR-WT mice [PAFR-WT: 0.96 ± 0.15 pg/mg tissue ($n = 4$) versus PAFR-KO: 1.16 ± 0.39 pg/mg tissue ($n = 4$)] and increased by administration of FA, especially at day 14 in PAFR-WT mice [PAFR-WT at day 14, 11.08 ± 3.38 pg/mg tissue ($n = 4$) versus PAFR-WT normal kidney; $P < 0.05$] (Figure 11). The PAF levels in PAFR-WT mice were higher than those in PAFR-KO mice, especially at day 14, but those differences were not statistically significant.

PAF-Induced Chemotaxis in Macrophage

Infiltration of F4/80-positive macrophages in interstitial fibrosis of the kidney was attenuated in PAFR-KO mice; PAF is also known as a potent chemoattractant for leukocytes. For that reason, we examined the direct chemotactic activity of macrophages to PAF using a Boyden chamber system. Macrophages isolated from PAFR-WT mice showed a remarkable chemotactic activity to PAF at concentrations of 1 and 10 nmol/L. On the other hand, PAF induced no chemotaxis in macrophages isolated from PAFR-KO mice (Figure 12).

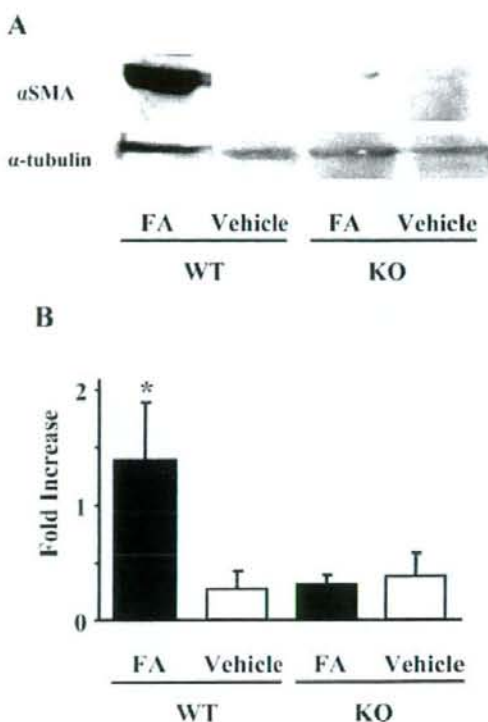


Figure 8. Western blot analysis of α -SMA expression in kidney homogenates at day 14. A representative image is depicted in **A** (top). **B:** The histogram illustrates the relative density of bands in comparison with α -tubulin. Five animals were in the FA group, four received the vehicle. * $P < 0.05$ versus PAFR-KO mice with FA administration.

Discussion

This study demonstrated that FA-induced renal injury comprises an acute and a subsequent chronic phase. Infiltration of ROS-producing neutrophils in acute tubular damage and macrophages in chronic interstitial fibrosis was attenuated significantly in PAFR-KO mice in comparison with PAFR-WT mice. Moreover, treatments of PAFR-WT mice with neutrophil depletion antibody and PAFR antagonist, which were started after the acute phase, also showed significant amelioration of acute tubular damage and macrophage infiltration and interstitial fibrosis in the chronic phase. Therefore, our data indicate that leukocytes play a crucial role both in the acute phase and the chronic phase of this animal model and that PAF is involved in pathogenesis of FA-induced inflammatory renal injury. To our knowledge, this study is the first to demonstrate the attenuation of renal injury in PAFR-KO mice, although several precedent studies have shown the effects of PAFR antagonists on renal disease in animal models.¹⁰⁻¹² However, those studies using PAFR antagonists often include problems related to drug specificity. Some PAFR antagonists inhibit the effect of histamine through interaction with its G protein-coupled receptor^{13,15}; other antagonists inhibit the activity of PAF

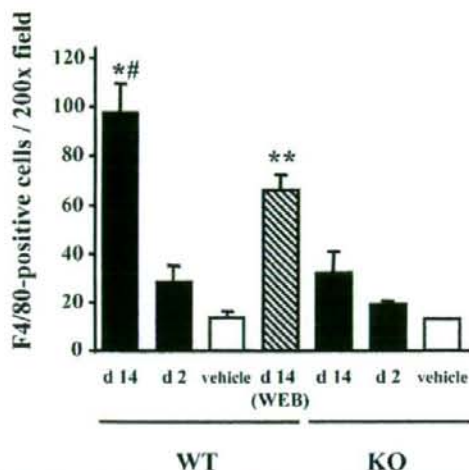


Figure 9. Number of infiltrating F4/80-positive cells in the tubulointerstitium with FA-induced renal injury. Five animals were in the FA group; four received the vehicle. * $P < 0.005$ versus PAFR-KO mice at day 14 (d 14). # $P < 0.05$ versus WEB2086-treated PAFR-WT mice at day 14. ** $P < 0.05$ versus PAFR-WT mice at day 14.

acetylhydrolase, which inactivates PAF.^{14,16} The present study demonstrates the pathological role of PAF in FA-induced renal injury using genetically engineered mice in which PAFR signaling was decreased congenitally by disrupting the PAFR gene. Several reports have used PAFR-KO mice to elucidate the role of PAF in various pathophysiological. The PAFR-KO mice exhibited attenuation in animal models in which inflammatory injuries were crucial: chemical lung injury,¹⁸ bronchial asthma,¹⁹ and sponge-induced subcutaneous granuloma formation.²⁰ On the other hand, PAFR-KO mice showed exacerbation of infection models such as pulmonary gram-negative bacteria infection⁴¹ and cardiac *Trypanosoma* infection.⁴² Those reports, along with the present study, indicate that PAF causes both beneficial and deleterious effects by activating leukocytes in different circumstances.

The neutrophil infiltration and lipid peroxidation of HHE in kidney at day 2 in PAFR-KO mice were significantly lower than those of PAFR-WT mice in this study. Stimulation of neutrophils with PAF *in vitro* engenders numerous cellular responses including chemotaxis,⁴³⁻⁴⁵ degranulation,⁴⁶ and ROS production.^{43,47} Priming neutrophils with PAF enhances ROS production by NADPH oxidase, which catalyzes superoxide production.⁴⁸ Through *in vivo* analysis with ischemia-reperfusion kidney injury, Kelly and colleagues⁴⁹ showed that PAFR antagonist reduced neutrophil infiltration. Lloberas and colleagues⁵⁰ showed that antioxidant treatment with vitamin C decreased PAF release from kidney and neutrophil infiltration to kidney. Moreover, neutrophil depletion by a monoclonal antibody RB6-8C5 significantly ameliorated FA-induced acute tubular damage in this study. These findings indicate that ROS produced by activated infiltrating neutrophils play an important role in FA-induced acute tubular damage. On the other hand, incomplete recovery of FA-induced

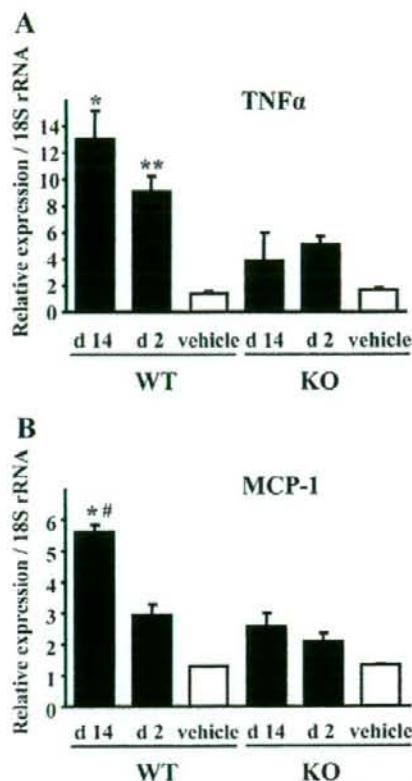


Figure 10. Quantitative analyses of expression of TNF- α (A) and MCP-1 (B) using real-time PCR. Eight animals were in the FA group; three received the vehicle. **A:** TNF- α expression was higher in PAFR-WT mice, both at days 2 and 14. * $P < 0.005$ versus PAFR-KO mice at day 14 (d 14), ** $P < 0.05$ versus PAFR-KO mice at day 2 (d 2). **B:** MCP-1 expression was higher in PAFR-WT mice than in PAFR-KO mice at day 14. * $P < 0.05$ versus PAFR-KO mice at day 14. Moreover, MCP-1 expression increased in PAFR-WT mice at day 14 greater than that at day 2. * $P < 0.05$ versus PAFR-WT mice at day 2.

renal injury in PAFR-KO mice and better improvement in neutrophil-depleted PAFR-WT mice than PAFR-KO mice, despite the lack of statistical difference between them, indicates that additional factors related to neutrophil activation might contribute to FA-induced injury.

Recruitment and activation of macrophages and lymphocytes to the kidney play a central role in a final pathway of most injuries to chronic kidney damage. Therefore, regulating these immunocompetent cells might be a potential target for therapeutic intervention for kidney disease.⁴ The PAFR-KO mice showed significant amelioration of FA-induced renal injury that developed to remarkable interstitial fibrosis with macrophage infiltration accompanied by the increase in the expression of TNF- α and MCP-1. Contribution of TNF- α for interstitial fibrosis was demonstrated in unilateral ureter obstruction, another renal fibrosis model, with TNF- α receptor knockout mice.⁵¹ In PAFR-KO mice, reduced macrophage infiltration number and lack of a PAF receptor pathway might engender decreased TNF- α expression in the kidney and

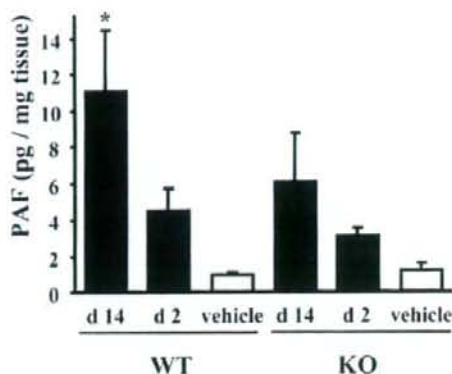


Figure 11. PAF level in FA-injured kidney. Four animals were in each group. * $P < 0.05$ versus PAFR-WT mice receiving the vehicle.

subsequent interstitial fibrosis. MCP-1 is presumed to play a potent role in macrophage chemotaxis and activation. Decreased expression of MCP-1 in PAFR-KO mice was in accordance with attenuated macrophage infiltration. MCP-1 production has been reported in tubular epithelial cells in unilateral ureter obstruction model⁵² and cultured renal proximal tubular epithelial cells.⁵³ We also found MCP-1 production in tubular epithelial cells by immunohistochemistry that was decreased in PAFR-KO mice. Furthermore, PAF activates nuclear factor- κ B,⁵⁴ which is critical for production of MCP-1 in tubular epithelial cells.⁵⁵ Expression of PAFR has been demonstrated in microdissected rat tubular cells⁵⁶ and tubular cell line LLC-PK1.⁵⁷ Taken together, it is quite plausible that PAF causes MCP-1 production in renal tubular cells. Indeed, Jocks and colleagues⁵⁸ showed MCP-1 induction by PAF in glomerular immune injury model with isolated perfused rat kidney. Beaudoux and colleagues⁵⁹ showed that PAF stimulated MCP-1 release in monocytes isolated from human peripheral blood. Further examination is required to clarify the role of PAF receptor pathway in renal tubular cells in this model.

We further examined the effect of blocking the PAF receptor pathway on macrophage recruitment with PAFR antagonist WEB2086 *in vivo*. It is noteworthy that treatment with WEB2086, even after acute tubular injury, also attenuated macrophage infiltration and interstitial fibrosis. Because we showed the chemotaxis activity of PAF to macrophages by Boyden chamber chemotaxis assay, PAF is likely to have a direct effect on the recruitment of macrophages to the injured kidney. However, renal functions and macrophage infiltration were not improved by WEB2086 to the degree of those of PAFR-KO mice. This might be because the degree of initial injury was so severe that WEB2086 could not improve renal function. Alternatively, WEB2086 could not suppress the PAF receptor pathway completely in this injury because of unfavorable pharmacokinetics and pharmacodynamics. Although several reports have described the effects of a single injection of WEB2086 at the dose of 5 to 10 mg/kg on mouse inflammation models,^{60,61} the optimal administration dose for chronic animal models and renal dys-

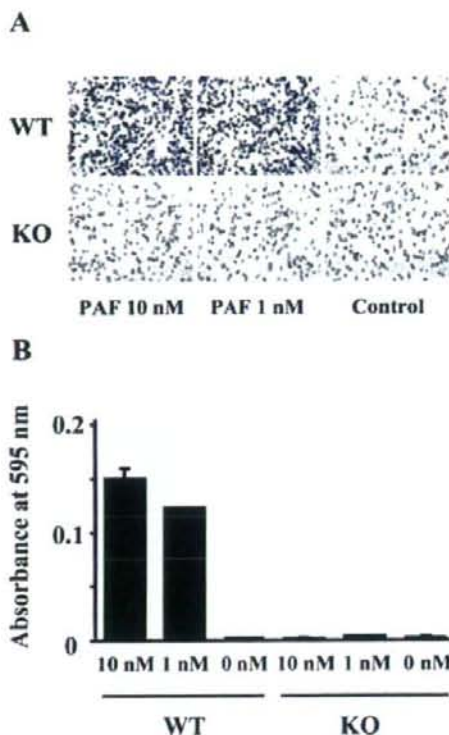


Figure 12. PAF-induced chemotaxis in elicited peritoneal macrophages harvested from PAFR-KO and PAFR-WT mice. **A:** Light microscope analysis of the migration toward PAF in the Boyden chamber assay. **B:** Quantitative analysis with measured absorbance at 595 nm. Each experiment was performed in triplicate. Original magnifications, $\times 200$.

function models remains unclear. Further evaluation is required for effects of WEB2086 on FA-induced renal injury.

We measured PAF levels in the kidney and found higher PAF levels in the kidneys of PAFR-WT mice than in those of PAFR-KO mice. This result indicated that there was an additional portion of PAF produced by oxidative stress secondary to initial injury and this component was decreased in PAFR-KO mice. We also found higher PAF levels at the chronic phase (day 14) than in the acute phase (day 2), especially in PAFR-WT mice. Changes of PAF levels in the kidney were similar to those of macrophage counts and MCP-1 expression. Therefore, it is plausible that PAF produced by initial injury enhanced macrophage infiltration to the kidney through MCP-1 expression and that the recruited macrophages produced PAF in the kidney. Our data indicate a vicious cycle of an amplifying effect of macrophage recruitment that is exacerbated by the PAF pathway.

The present study demonstrates the involvement of PAF in FA-induced renal inflammatory injury. Blockade of the PAF receptor pathway significantly attenuates both acute tubular damage and subsequent chronic development of interstitial fibrosis by reducing infiltrating leuko-

cytes. Such a blockade suggests a potent therapeutic approach to kidney injury caused by inflammatory cells.

Acknowledgments

We thank Dr. R. Coffman (DNAX Research Inc., Palo Alto, CA) for providing RB6-8C5 hybridoma and Ms. Mami Haba for her skilled assistance.

References

- Schrier RW, Wang W, Poole B, Mitra A: Acute renal failure: definitions, diagnosis, pathogenesis, and therapy. *J Clin Invest* 2004, 114:5-14
- Bonventre JV, Zuk A: Ischemic acute renal failure: an inflammatory disease? *Kidney Int* 2004, 66:480-485
- Strutz F, Neilson EG: The role of lymphocytes in the progression of interstitial disease. *Kidney Int Suppl* 1994, 45:S106-S110
- Rodriguez-Isturbe B, Pons H, Herrera-Acosta J, Johnson RJ: Role of immunocompetent cells in nonimmune renal diseases. *Kidney Int* 2001, 59:1626-1640
- Ishii S, Shimizu T: Platelet-activating factor (PAF) receptor and genetically engineered PAF receptor mutant mice. *Prog Lipid Res* 2000, 39:41-82
- Imazumi TA, Stafforini DM, Yamada Y, McIntyre TM, Prescott SM, Zimmerman GA: Platelet-activating factor: a mediator for clinicians. *J Intern Med* 1995, 238:5-20
- Blank ML, Snyder F, Byers LW, Brooks B, Muirhead EE: Antihypertensive activity of an alkyl ether analog of phosphatidylcholine. *Biochem Biophys Res Commun* 1979, 90:1194-1200
- Lopez-Farre A, Torralba M, Lopez-Novoa JM: Glomeruli from ischemic rat kidneys produce increased amounts of platelet activating factor. *Biochem Biophys Res Commun* 1988, 152:129-135
- Takahashi S, Imaigawa M, Mirmata H, Nakagawa M, Ogata J, Nomura Y: Role of platelet-activating factor in two-kidney, one-clip hypertension. *Int J Urol* 1997, 4:388-393
- Lopez-Novoa JM: Potential role of platelet activating factor in acute renal failure. *Kidney Int* 1999, 55:1672-1682
- Thaiss F, Mihatsch MJ, Oberle G, Haberstroh U, Brecht HM, Stahl RA: Platelet-activating factor receptor antagonist improves renal function and glomerular lesions in renal ablation. *J Lab Clin Med* 1994, 124:775-781
- Torras J, Cruzado JM, Riera M, Condom E, Duque N, Herrero I, Merlos M, Espinosa L, Lloberas N, Egido J, Grinyo JM: Long-term protective effect of UR-12670 after warm renal ischemia in uninephrectomized rats. *Kidney Int* 1999, 56:1798-1806
- Carceller E, Merlos M, Girai M, Balsa D, Almansa C, Bartoli J, Garcia-Rafanell J, Forn J: [(3-Pyridylalkyl)pyperidylidene]benzocycloheptapyridine derivatives as dual antagonists of PAF and histamine. *J Med Chem* 1994, 37:2697-2703
- Svetlov SI, Howard KM, Miwa M, Flickinger BD, Olson MS: Interaction of platelet-activating factor with rat hepatocytes: uptake, translocation, metabolism, and effects on PAF-acetylhydrolase secretion and protein tyrosine phosphorylation. *Arch Biochem Biophys* 1996, 327:113-122
- Merlos M, Girai M, Balsa D, Ferrando R, Queralt M, Puigdemont A, Garcia-Rafanell J, Forn J: Rupatadine, a new potent, orally active dual antagonist of histamine and platelet-activating factor (PAF). *J Pharmacol Exp Ther* 1997, 280:114-121
- Adachi T, Aoki J, Manya H, Asou H, Arai H, Inoue K: PAF analogues capable of inhibiting PAF acetylhydrolase activity suppress migration of isolated rat cerebellar granule cells. *Neurosci Lett* 1997, 235:133-136
- Ishii S, Kuwaki T, Nagase T, Maki K, Tashiro F, Sunaga S, Cao WH, Kume K, Fukuchi Y, Ikuta K, Miyazaki J, Kumada M, Shimizu T: Impaired anaphylactic responses with intact sensitivity to endotoxin in mice lacking a platelet-activating factor receptor. *J Exp Med* 1998, 187:1779-1788
- Nagase T, Ishii S, Kume K, Uozumi N, Izumi T, Ouchi Y, Shimizu T: Platelet-activating factor mediates acid-induced lung injury in genetically engineered mice. *J Clin Invest* 1999, 104:1071-1078

- Ishii S, Nagase T, Shindou H, Takizawa H, Ouchi Y, Shimizu T: Platelet-activating factor receptor develops airway hyperresponsiveness independently of airway inflammation in a murine asthma model. *J Immunol* 2004, 172:7095-7102
- Ferreira MA, Barcelos LS, Campos PP, Vasconcelos AC, Teixeira MM, Andrade SP: Sponge-induced angiogenesis and inflammation in PAF receptor-deficient mice (PAFR-KO). *Br J Pharmacol* 2004, 141:1185-1192
- Long DA, Woolf AS, Suda T, Yuan HT: Increased renal angiotensin-1 expression in folic acid-induced nephrotoxicity in mice. *J Am Soc Nephrol* 2001, 12:2721-2731
- Surendran K, McCaul SP, Simon TC: A role for Wnt-4 in renal fibrosis. *Am J Physiol* 2002, 282:F431-F441
- Yuan HT, Li XZ, Pitera JE, Long DA, Woolf AS: Peritubular capillary loss after mouse acute nephrotoxicity correlates with down-regulation of vascular endothelial growth factor-A and hypoxia-inducible factor-1 alpha. *Am J Pathol* 2003, 163:2289-2301
- Surendran K, Simon TC, Liapis H, McGuire JK: Matrilysin (MMP-7) expression in renal tubular damage: association with Wnt4. *Kidney Int* 2004, 65:2212-2222
- Byrnes KA, Ghidoni JJ, Suzuki M, Thomas H, Mayfield Jr ED: Response of the rat kidney to folic acid administration. II. Morphologic studies. *Lab Invest* 1972, 26:191-200
- Fink M, Henry M, Tange JD: Experimental folic acid nephropathy. *Pathology* 1987, 19:143-149
- Rogers HW, Unanue ER: Neutrophils are involved in acute, nonspecific resistance to *Listeria monocytogenes* in mice. *Infect Immun* 1993, 61:5090-5096
- Conlan JW, North RJ: Neutrophils are essential for early anti-*Listeria* defense in the liver, but not in the spleen or peritoneal cavity, as revealed by a granulocyte-depleting monoclonal antibody. *J Exp Med* 1994, 179:259-268
- Czuprynski CJ, Brown JF, Wagner RD, Steinberg H: Administration of antigranulocyte monoclonal antibody RB6-8C5 prevents expression of acquired resistance to *Listeria monocytogenes* infection in previously immunized mice. *Infect Immun* 1994, 62:5161-5163
- Czuprynski CJ, Brown JF, Maroushek N, Wagner RD, Steinberg H: Administration of anti-granulocyte mAb RB6-8C5 impairs the resistance of mice to *Listeria monocytogenes* infection. *J Immunol* 1994, 152:1836-1846
- Rakhmievich AL: Neutrophils are essential for resolution of primary and secondary infection with *Listeria monocytogenes*. *J Leukoc Biol* 1995, 57:827-831
- Chen L, Zhang Z, Sento F: Neutrophils play a critical role in the pathogenesis of experimental cerebral malaria. *Clin Exp Immunol* 2000, 120:125-133
- Chen L, Watanabe T, Watanabe H, Sento F: Neutrophil depletion exacerbates experimental Chagas' disease in BALB/c, but protects C57BL/6 mice through modulating the Th1/Th2 dichotomy in different directions. *Eur J Immunol* 2001, 31:265-275
- Stephans-Romero SD, Mednick AJ, Feldmesser M: The pathogenesis of fatal outcome in murine pulmonary aspergillosis depends on the neutrophil depletion strategy. *Infect Immun* 2005, 73:114-125
- Doi K, Suzuki Y, Nakao A, Fujita T, Noiri E: Radical scavenger edaravone developed for clinical use ameliorates ischemia/reperfusion injury in rat kidney. *Kidney Int* 2004, 65:1714-1723
- Ohse T, Ota T, Kieran N, Godson C, Yamada K, Tanaka T, Fujita T, Nangaku M: Modulation of interferon-induced genes by lipoxin analogue in anti-glomerular basement membrane nephritis. *J Am Soc Nephrol* 2004, 15:919-927
- Hisada Y, Sugaya T, Yamanouchi M, Uchida H, Fujimura H, Sakurai H, Fukamizu A, Murakami K: Angiotensin II plays a pathogenic role in immune-mediated renal injury in mice. *J Clin Invest* 1999, 103:627-635
- Kihara Y, Ishii S, Kita Y, Toda A, Shimada A, Shimizu T: Dual phase regulation of experimental allergic encephalomyelitis by platelet-activating factor. *J Exp Med* 2005, 202:853-863
- Kita Y, Takahashi T, Uozumi N, Shimizu T: A multiplex quantitation method for eicosanoids and platelet-activating factor using column-switching reversed-phase liquid chromatography-tandem mass spectrometry. *Anal Biochem* 2005, 342:134-143
- Yokomizo T, Izumi T, Chang K, Takuwa Y, Shimizu T: A G-protein-coupled receptor for leukotriene B4 that mediates chemotaxis. *Nature* 1997, 387:620-624

41. Soares AC, Pinho VS, Souza DG, Shimizu T, Ishii S, Nicoli JR, Teixeira MM: Role of the platelet-activating factor (PAF) receptor during pulmonary infection with gram negative bacteria. *Br J Pharmacol* 2002, 137:621-628
42. Talvani A, Santana G, Barcelos LS, Ishii S, Shimizu T, Romanha AJ, Silva JS, Soares MB, Teixeira MM: Experimental *Trypanosoma cruzi* infection in platelet-activating factor receptor-deficient mice. *Microbes Infect* 2003, 5:789-796
43. Ingraham LM, Coates TD, Allen JM, Higgins CP, Baehner RL, Boxer LA: Metabolic, membrane, and functional responses of human polymorphonuclear leukocytes to platelet-activating factor. *Blood* 1982, 59:1259-1266
44. Gaudreault E, Stankova J, Rola-Pleszczynski M: Involvement of leukotriene B4 receptor 1 signaling in platelet-activating factor-mediated neutrophil degranulation and chemotaxis. *Prostaglandins Other Lipid Mediat* 2005, 75:25-34
45. Gambero A, Thomazzi SM, Cintra AC, Landucci EC, De Nucci G, Antunes E: Signalling pathways regulating human neutrophil migration induced by secretory phospholipases A2. *Toxicol* 2004, 44:473-481
46. O'Flaherty JT, Swendsen CL, Lees CJ, McCall CE: Role of extra cellular calcium and neutrophil degranulation responses to 1-O-alkyl-2-O-acetyl-sn-glycero-3-phosphocholine. *Am J Pathol* 1981, 105:107-113
47. Elzi DJ, Hiestar AA, Silliman CC: Receptor-mediated calcium entry is required for maximal effects of platelet activating factor primed responses in human neutrophils. *Biochem Biophys Res Commun* 1997, 240:763-765
48. Vercellotti GM, Yin HQ, Gustafson KS, Nelson RD, Jacob HS: Platelet-activating factor primes neutrophil responses to agonists: role in promoting neutrophil-mediated endothelial damage. *Blood* 1988, 71:1100-1107
49. Kelly KJ, Tolkoff-Rubin NE, Rubin RH, Williams Jr WW, Meehan SM, Meschter CL, Christenson JG, Bonventre JV: An oral platelet-activating factor antagonist, Ro-24-4736, protects the rat kidney from ischemic injury. *Am J Physiol* 1996, 271:F1061-F1067
50. Lloberas N, Torras J, Herrero-Fresneda I, Cruzado JM, Riera M, Hurtado I, Grinyo JM: Postischemic renal oxidative stress induces inflammatory response through PAF and oxidized phospholipids. Prevention by antioxidant treatment. *FASEB J* 2002, 16:908-910
51. Guo G, Morrissey J, McCracken R, Tolley T, Klahr S: Role of TNFR1 and TNFR2 receptors in tubulointerstitial fibrosis of obstructive nephropathy. *Am J Physiol* 1999, 277:F766-F772
52. Kitagawa K, Wada T, Furuichi K, Hashimoto H, Ishiwata Y, Asano M, Takaya M, Kuziel WA, Matsushima K, Mukaida N, Yokoyama H: Blockade of CCR2 ameliorates progressive fibrosis in kidney. *Am J Pathol* 2004, 165:237-246
53. Takaya K, Koya D, Isono M, Sugimoto T, Sugaya T, Kashiwagi A, Haneda M: Involvement of ERK pathway in albumin-induced MCP-1 expression in mouse proximal tubular cells. *Am J Physiol* 2003, 284:F1037-F1045
54. Kravchenko VV, Pan Z, Han J, Herbert JM, Ulevitch RJ, Ye RD: Platelet-activating factor induces NF-kappa B activation through a G protein-coupled pathway. *J Biol Chem* 1995, 270:14928-14934
55. Wang Y, Rangan GK, Goodwin B, Tay YC, Harris DC: Lipopolysaccharide-induced MCP-1 gene expression in rat tubular epithelial cells is nuclear factor-kappaB dependent. *Kidney Int* 2000, 57:2011-2022
56. Asano K, Taniguchi S, Nakao A, Watanabe T, Kurokawa K: Distribution of platelet activating factor receptor mRNA along the rat nephron segments. *Biochem Biophys Res Commun* 1996, 225:352-357
57. Jamil KM, Takano T, Nakao A, Honda Z, Shimizu T, Watanabe T, Kurokawa K: Expression of platelet activating factor receptor in renal tubular cell line (LLC-PK1). *Biochem Biophys Res Commun* 1992, 187:767-772
58. Jocks T, Freudenberg J, Zahner G, Stahl RA: Platelet-activating factor mediates monocyte chemoattractant protein-1 expression in glomerular immune injury. *Nephrol Dial Transplant* 1998, 13:37-43
59. Beaudaux JL, Said T, Ninio E, Ganne F, Soria J, Delattre J, Soria C, Lagrand A, Peynet J: Activation of PAF receptor by oxidised LDL in human monocytes stimulates chemokine releases but not urokinase-type plasminogen activator expression. *Clin Chim Acta* 2004, 344:163-171
60. Getting SJ, Flower RJ, Parente L, de Medicis R, Lussier A, Wolitzky BA, Martins MA, Perretti M: Molecular determinants of monosodium urate crystal-induced murine peritonitis: a role for endogenous mast cells and a distinct requirement for endothelial-derived selectins. *J Pharmacol Exp Ther* 1997, 283:123-130
61. Perretti M, Flower RJ: Modulation of IL-1-induced neutrophil migration by dexamethasone and lipocortin 1. *J Immunol* 1993, 150:992-999

長寿科学総合研究事業

高齢者呼吸器疾患の発症・制御に関与する遺伝子
・蛋白系の解明と治療応用に関する研究

平成18年度～平成20年度 総合研究報告書

発行 平成21年3月31日

発行者 「高齢者呼吸器疾患の発症・制御に関与する遺伝子
・蛋白系の解明と治療応用」

研究代表者 長瀬 隆英
〒113-8655
東京都文京区本郷 7-3-1
東京大学医学部附属病院